

# Fourier Beyond Dispersion: Wavenumber Explicit and Precise Accuracy of FDMs for the Helmholtz Equation

Hui Zhang\*

School of Mathematics and Physics, Xi'an Jiaotong-Liverpool University, Ren'ai Rd. 111, Suzhou 215123, China  
Email: hui.zhang@xjtlu.edu.cn

December 18, 2024

## Abstract

We propose a practical tool for evaluating and comparing the accuracy of FDMs for the Helmholtz equation. The tool based on Fourier analysis makes it easy to find wavenumber explicit order of convergence, and can be used for rigorous proof. It fills in the gap between the dispersion analysis and the actual error with source term.

**Keywords** Fourier analysis, finite difference, Helmholtz equation, dispersion analysis, pollution effect  
**MSC 2020** 65N06, 65N12, 65N15

## 1 Introduction.

Discretization of the Helmholtz equation suffers from the ‘pollution effect’: “the accuracy of the numerical solution deteriorates with increasing non-dimensional wave number  $k$ ” [3]. It is related to that the numerical solution “has a wavelength that is different from the exact one” [3] called ‘dispersion’. Albeit useful [2, 6, 8], dispersion analysis [3] has not a trivial path to the total error estimate [1] with source term. In particular, the wavenumber explicit estimate is largely missing in the FDM literature [5, 7]. Inspired by [4], we propose a Fourier analysis approach to precise error estimation. We shall illustrate the approach in 1D. But it is applicable in 2D and 3D. It also provides a framework for rigorous proof of sharp error estimates. Those extensions will appear elsewhere.

## 2 Analysis in 1D

We consider the model problem with homogeneous Dirichlet boundary condition

$$\mathcal{H}u := u'' + k^2u = f \text{ in } \Omega := (0, 1), \quad u(0) = u(1) = 0. \quad (1) \text{ helm1d}$$

We assume  $f \in H_0^p(0, 1)$ ,  $p \geq 1$  and  $k \notin \pi\mathbb{Z}$ . Then (1) has a unique solution  $u \in H^{p+2}(0, 1) \cap H_0^1(0, 1)$ . It holds

$$f(x) = \sum_{n=1}^{\infty} \hat{f}_n \sin(n\pi x), \quad \hat{f}_n := 2 \int_0^1 f(x) \sin(n\pi x) dx, \quad u(x) = \sum_{n=1}^{\infty} \hat{u}_n \sin(n\pi x), \quad \hat{u}_n := 2 \int_0^1 u(x) \sin(n\pi x) dx.$$

From the equation (1), we get  $\hat{u}_n = \frac{1}{k^2 - \xi_n^2} \hat{f}_n =: \hat{\mathcal{H}}_n^{-1} \hat{f}_n$  where  $\xi_n = n\pi$ .

We discretize the domain  $(0, 1)$  into the uniform grids  $\Omega_h := \{x_j = jh, j = 1, \dots, N-1\}$  with  $h = \frac{1}{N}$  and  $N \geq 4$  an integer. Denote a finite difference scheme by  $\mathcal{H}^h u^h = \mathcal{R}^h f =: f^h$  where  $u^h$  and  $\mathcal{R}^h f$  are functions on  $\Omega_h$ . We have the discrete Fourier transform

$$\begin{aligned} f^h(x) &= \sum_{n=1}^{N-1} \hat{f}_n^h \sin(n\pi x), & \hat{f}_n^h &:= \frac{2}{N} \sum_{j=1}^{N-1} f^h(x_j) \sin(n\pi x_j), \\ u^h(x) &= \sum_{n=1}^{N-1} \hat{u}_n^h \sin(n\pi x), & \hat{u}_n^h &:= \frac{2}{N} \sum_{j=1}^{N-1} u^h(x_j) \sin(n\pi x_j), \end{aligned} \quad (2) \text{ uh}$$

where the formulae of  $f^h(x)$  and  $u^h(x)$  hold originally for  $x \in \Omega_h$  but is also used for extended definition of  $f^h(x)$  and  $u^h(x)$  at  $x \in \Omega = (0, 1)$ . From  $\mathcal{H}^h u^h = f^h$ , we shall be able to find  $\hat{u}_n^h = (\hat{\mathcal{H}}_n^h)^{-1} \hat{f}_n^h$ . The error  $u - u^h$  is then

$$u - u^h = \sum_{n=1}^{N-1} (\hat{u}_n - \hat{u}_n^h) \sin(n\pi x) + \sum_{n=N}^{\infty} \hat{u}_n \sin(n\pi x).$$

For simplicity, we assume the source  $f$  is well resolved on  $\Omega_h$  i.e.  $f$  is band limited with  $\hat{f}_n = 0$  for  $n \geq N$ . It follows that  $f$  and its first and high order derivatives have the Fourier expansion

$$f(x) = \sum_{n=1}^{N-1} \hat{f}_n \sin(n\pi x), \quad f^{(2q)}(x) = \sum_{n=1}^{N-1} (-\xi_n^2)^q \hat{f}_n \sin(n\pi x), \quad f^{(2q+1)}(x) = \sum_{n=1}^{N-1} (-1)^q \xi_n^{2q+1} \hat{f}_n \cos(n\pi x), \quad \xi_n = n\pi.$$

An analysis including under resolved  $f$  will appear elsewhere. For band limited  $f$ , the error becomes

$$u - u^h = \sum_{n=1}^{N-1} (\hat{u}_n - \hat{u}_n^h) \sin(n\pi x) = \sum_{n=1}^{N-1} \left( \hat{\mathcal{H}}_n^{-1} - (\hat{\mathcal{H}}_n^h)^{-1} \hat{\mathcal{R}}_n^h \right) \hat{f}_n \sin(n\pi x), \quad (3) \quad \boxed{\text{err1d}}$$

where the Fourier transform of  $\mathcal{R}^h f$  is supposed to be  $\widehat{(\mathcal{R}^h f)}_n = \hat{\mathcal{R}}_n^h \hat{f}_n$ .

**Theorem 1.** *Suppose  $k \notin \pi\mathbb{Z}$ ,  $f \in H_0^p(0,1)$  and  $f$  is band limited with the Fourier coefficients  $\hat{f}_n = 0$  for  $n \geq N$  for an even integer  $N \geq 4$ . Let  $u$  be the solution of (1). Suppose a linear finite difference equation  $\hat{\mathcal{H}}^h u^h = \mathcal{R}^h f$  on  $\Omega_h$  with  $u^h(0) = u^h(1) = 0$  has a unique solution  $u^h$ , where  $\Omega_h := \{x_j = jh, j = 1, \dots, N-1\}$  and  $h = \frac{1}{N}$ . Let  $u^h$  be extended by the discrete Fourier transform to  $\Omega = (0,1)$ . Then we have*

$$\|u - u^h\|_{L^2(0,1)} \leq \|f\|_{H^p(0,1)} \max_{n=1, \dots, N-1} \left| \hat{\mathcal{H}}_n^{-1} - (\hat{\mathcal{H}}_n^h)^{-1} \hat{\mathcal{R}}_n^h \right| / |\xi_n|^p,$$

$$|u - u^h|_{H^1(0,1)} \leq \|f\|_{H^p(0,1)} \max_{n=1, \dots, N-1} \left| \hat{\mathcal{H}}_n^{-1} - (\hat{\mathcal{H}}_n^h)^{-1} \hat{\mathcal{R}}_n^h \right| / |\xi_n|^{p-1},$$

where  $|v|_{H^p(0,1)} = \|v^{(p)}\|_{L^2(0,1)}$  is the  $H^p$ -semi-norm,  $\xi_n = n\pi$ , and both upper bounds are attainable.

*Proof.* The first inequality follows from the Parseval's identity in view of (3)

$$2\|u - u^h\|_{L^2(0,1)}^2 = \sum_{n=1}^{N-1} \left| \hat{\mathcal{H}}_n^{-1} - (\hat{\mathcal{H}}_n^h)^{-1} \hat{\mathcal{R}}_n^h \right|^2 |\hat{f}_n|^2.$$

The other inequalities can be proved in a similar way. □

**Remark 1.** *For an  $m$ th order scheme, we usually choose  $p = m - 2$  in Theorem 1. Sometimes, it is useful to choose  $p = m - 1$  for the  $H^1$ -semi-norm of the error. We shall see when  $p \geq 1$  the  $H^p$ -semi-norm of  $f$  does contribute extra powers of  $k$  to the upper bound, because 1) the upper bound is attained when  $\hat{f}_n$  is supported on the frequency where the maximum term in the upper bound is attained, and 2) the maximum term is often attained at a frequency near the wavenumber  $k$ . More precisely, if the upper bound is attained when  $f = \sin(\xi x)$  with  $\xi$  of order  $k$  then  $|f|_{H^p(0,1)}$  is of order  $k^p$ . Thus, we consider as hard as possible a Helmholtz problem for each wavenumber  $k$ .*

## 2.1 FDMs in 1D and their symbols

The baseline is of course the classical centered scheme

$$\mathcal{H}_{cls}^h u^h := \left(k^2 - \frac{2}{h^2}\right) u^h(x_j) + \frac{1}{h^2} u^h(x_{j-1}) + \frac{1}{h^2} u^h(x_{j+1}) = f(x_j), \quad x_j \in \Omega_h.$$

Its left hand side symbol is  $\hat{\mathcal{H}}_{cls,n}^h = k^2 - \frac{4}{h^2} \sin^2 \frac{\xi_n h}{2}$  with  $\xi_n = n\pi$ , and right hand side symbol is  $\hat{\mathcal{R}}_{cls,n}^h = 1$ . It is well known that the dispersion error in 1D is avoidable; see [1]. Arbitrarily high order 3-point schemes without dispersion in 1D was derived [7]. We shall study those schemes of order 2, 4, and 6. The 2nd order dispersion free scheme reads

$$\mathcal{H}_{df}^h u^h := k^2 u^h(x_j) + \frac{k^2}{\tilde{k}^2} \left[ -\frac{2}{h^2} u^h(x_j) + \frac{1}{h^2} u^h(x_{j-1}) + \frac{1}{h^2} u^h(x_{j+1}) \right] = f(x_j), \quad x_j \in \Omega_h,$$

where  $\tilde{k} = \frac{2}{h} \sin \frac{kh}{2}$ . Its left hand side symbol is  $\hat{\mathcal{H}}_{df,n}^h = k^2 - \frac{k^2}{\tilde{k}^2} \frac{4}{h^2} \sin^2 \frac{\xi_n h}{2}$ . The fourth order dispersion free scheme uses the same left hand side operator as the second order scheme uses but different right hand side operator:

$$\mathcal{H}_{df}^h u^h = f(x_j) + \left( \frac{1}{\tilde{k}^2} - \frac{1}{k^2} \right) f''(x_j) =: (\mathcal{R}_{df4}^h f)(x_j), \quad x_j \in \Omega_h.$$

Its right hand side symbol is  $\hat{\mathcal{R}}_{df4,n}^h = 1 - \xi_n^2 \left( \frac{1}{k^2} - \frac{1}{k^2} \right)$ . For the sixth order dispersion free scheme, the left hand side is the same as before, and the right hand side operator is

$$(\mathcal{R}_{df6}^h f)(x_j) = (\mathcal{R}_{df4}^h f)(x_j) + \left[ \frac{1}{k^4} + \left( \frac{h^2}{12} - \frac{1}{k^2} \right) \frac{1}{k^2} \right] f^{(4)}(x_j).$$

So its symbol is  $\hat{\mathcal{R}}_{df6,n}^h = \hat{\mathcal{R}}_{df4,n}^h + \xi_n^4 \left( \frac{h^2}{12} - \frac{1}{k^2} \right) \frac{1}{k^2}$ .

## 2.2 Accuracy of FDMs in 1D

(acc) According to (3) and Theorem 1, the error is essentially determined by

$$\psi_p(\xi_n) := \left| \hat{\mathcal{H}}_n^{-1} - (\hat{\mathcal{H}}_n^h)^{-1} \hat{\mathcal{R}}_n^h \right| / |\xi_n|^p, \quad \xi_n = n\pi, \quad n = 1, \dots, N-1.$$

Recall Remark 1 that if  $\max_n \psi_p(\xi_n)$  for the  $L^2$ -norm error, or  $\max_n \psi_{p-1}(\xi_n)$  for the  $H^1$ -semi-norm error, is attained near  $k$  then  $|f|_{H^p(0,1)}$  will be of order  $k^p$ . In that case, we shall multiply  $\psi_p$  or  $\psi_{p-1}$  with  $k^p$  to represent (up to a constant factor) the sharp upper bound of the  $L^2$ -norm or  $H^1$ -semi-norm error. This gives rise to Fig. 1 for the FDMs described in Sect. 2.1, where  $p = m - 2$  is used for an  $m$ th order (in  $h$ ) scheme. In the first (second) column of the figure, we show  $\psi_p$  ( $\psi_{p-1}$ ) for  $L^2$ - ( $H^1$ -semi-) norm error, from which, we can see clearly how the error is distributed over the Fourier frequencies  $\xi_n$ . In particular, all  $\max_n \psi_p$  are attained at a  $\xi_n$  near  $k$ . In the third column, we present the scaling results of  $k^p \max \psi$ .

The first row illustrates the convergence of classical scheme in term of  $h$ -refinement with fixed  $k$ , which confirms the order  $O(h^2)$  for both  $L^2$ - (indicated by  $\max \psi_0$ ) and  $H^1$ -semi- (indicated by  $\max \psi_{-1}$ ) norms of the error. Since the order in  $h$  is well-known, we shall not illustrate that for the other schemes.

The second row is again for the classical scheme, but  $k$  doubles while  $N = h^{-1}$  quadruples. It is seen that  $\psi_{-1}$  converges slower than  $\psi_0$  in this setting. In particular, the subfigure in row 2 and column 3 shows that the order of  $L^2$ -norm error (indicated by  $\max \psi_0$ ) is  $k^2 h^2$  for the Fourier interpolated  $u^h$  in (2), while the plots for  $\max \psi_{-1}$  needs some explanation. While  $k$  doubles and  $h^{-1}$  quadruples simultaneously, it follows that  $kh$  halves, and  $\max \psi_{-1}$  halves (linear in  $kh$ ) seen from the subfigure. Since the order in  $h$  is 2, the order in  $k$  and  $h$  should be  $k^\alpha h^2$  for some  $\alpha$ . Since  $(2k)^\alpha (h/4)^2 = k^\alpha h^2 2^{\alpha-4}$ , we should have  $\alpha - 4 = -1$  i.e.  $\alpha = 3$  and the order of  $H^1$ -semi-norm error is  $k^3 h^2$ . The conclusion drawn here can be proved rigorously based on Theorem 1, which will appear elsewhere.

The other rows are for the dispersion free schemes [7] described in Sect 2.1. It is seen that the  $L^2$ -norm error converges faster than the  $H^1$ -semi-norm error in the setting that  $k$  doubles while  $h^{-1}$  quadruples. Since the order in  $h$  is known, the scaling with ‘wrong’ order in  $h$  in column 3 subfigures need some explanation. For the 2nd order scheme, the  $k^3 h^3$  scaling means  $k^2 \max \psi_0$  scales down by one eighth when  $k$  doubles and  $h$  quadruples simultaneously. So  $(2k)^\alpha (h/4)^2 = k^\alpha h^2 2^{\alpha-4}$  should have  $\alpha - 4 = -3$  i.e.  $\alpha = 1$  and the  $L^2$ -norm error is of order  $kh^2$ . Similarly, the 4th (6th) order scheme has the  $L^2$ -norm error of order  $k^3 h^4$  ( $k^5 h^6$ ) from  $\alpha - 8 = -5$  ( $\alpha - 12 = -7$ ).

## 3 Numerical experiments in 1D

We solve (1) numerically by the FDMs described in Sect. 2.1. Two different type of sources are used. With  $k = n_k \pi + 1$  and a monochromatic source  $f(x) = \sin(n_k \pi x)$ , the exact solution is  $u(x) = f(x)/(k^2 - n_k^2 \pi^2)$ . With a mixed source  $f(x) = \sum_{j=0}^5 \sin(2^j \times 5\pi x)$ , the exact solution is  $u(x) = \sum_{j=0}^5 \frac{1}{k^2 - 2^{2j} \times 25\pi^2} \sin(2^j \times 5\pi x)$ . A range of  $k$  and  $h$  values are tested. Denote the error  $e^h := u - u^h$ . The error (semi-)norms  $\|e^h\|_{L^2(0,1)}$  and  $|e^h|_{H^1(0,1)}$  are computed in the Fourier frequency domain by Parseval’s identity. The results are shown in Fig. 3.

In the first row of Fig. 3, the error of classical scheme is presented. For the source  $f(x) = \sin(k-1)x$  of a single frequency near the wavenumber  $k = n_k \pi + 1$ , the  $L^2$ -norm error in the first column is seen of order  $k^2 h^2$  with  $\|e^h\|_{L^2}/(k^2 h^2)$  almost independent of  $k$ , which corroborates Theorem 1. It is only when  $kh > 0.2$  that larger  $k$  leads to a smaller  $\|e^h\|_{L^2}$  at the same  $kh$  value. This preasymptotic behavior can be understood from the symbol error  $\psi_0(k-1) = \hat{\mathcal{H}}^{-1} - (\hat{\mathcal{H}}_{cls,n_k})^{-1} = \frac{1}{k^2 - (k-1)^2} - \frac{1}{k^2 - \frac{4}{h^2} \sin^2 \frac{(k-1)h}{2}}$  which is about 0.0106384, 0.00832166, 0.00558938, 0.00329617, 0.00180466 for  $k = 5\pi + 1, 10\pi + 1, 20\pi + 1, 40\pi + 1, 80\pi + 1$  at  $h = 1/\lceil k \rceil$ . The  $H^1$ -semi-norm error for the monochromatic source is shown in the second column. Along each line for a fixed  $k$ , the subfigure shows that  $|e^h|_{H^1}$  decays at the rate of order  $h^2$ . But at the same  $kh$  value, it shows that  $|e^h|_{H^1}$  doubles when  $k$  doubles, thus confirms

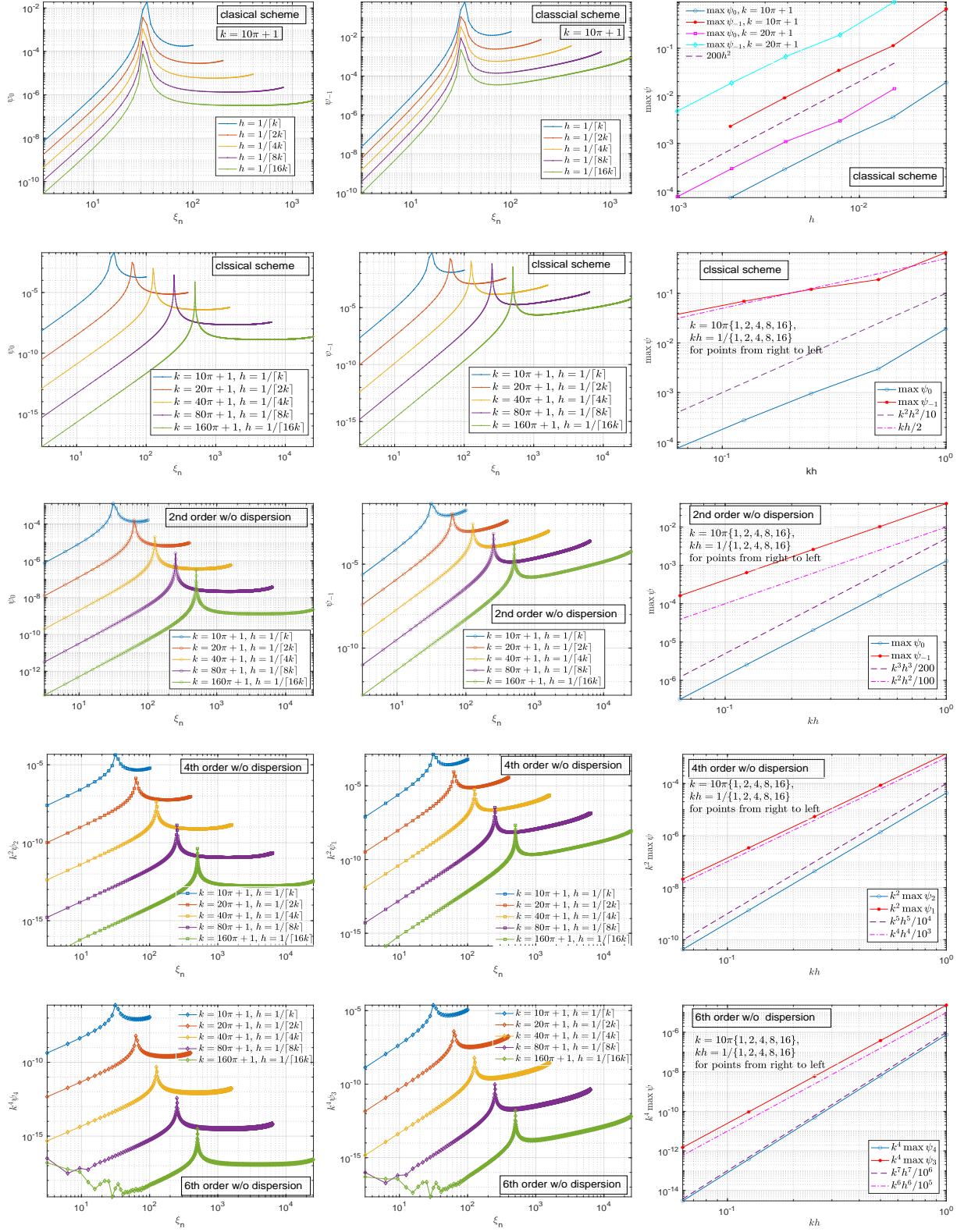


Figure 1: Symbol errors in 1D:  $k^p \psi_p$  for  $L^2$ -norm (col.1) and  $k^p \psi_{p-1}$  for  $H^1$ -semi-norm (col.2).

{1dfig}

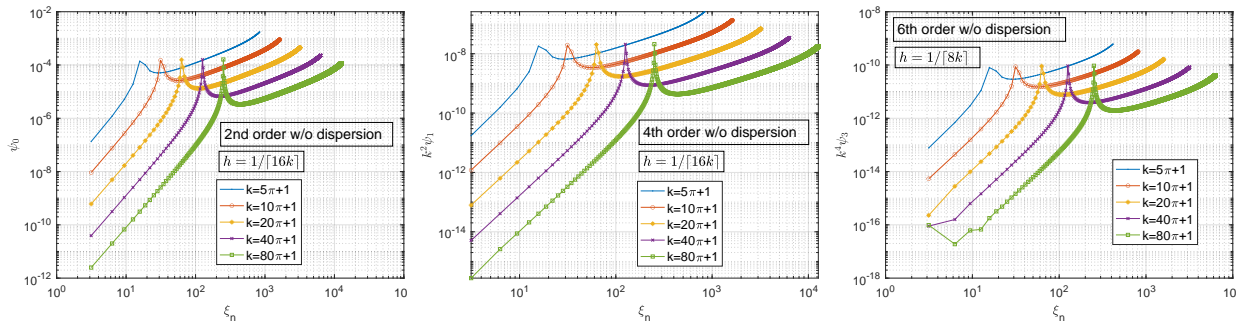


Figure 2: Symbol errors in 1D with  $kh$  fixed and  $k$  increases.

1dkhfixed)

the finding in Sect. 2.2 that  $|e^h|_{H^1}$  is of order  $k^3 h^2$ . The last two columns of the first row for the mixed and fixed source are similar to the first two columns for the monochromatic source, showing that the error is still concentrated at nearly resonant (i.e. near  $k$ ) Fourier frequencies.

In the second and subsequent rows of Fig. 3, the dispersion free schemes [7] described in Sect. 2.1 are studied. It is seen that, for both monochromatic and mixed sources, the  $L^2$ -norm error is of the expected order  $m$  in  $h$  and order  $m - 1$  in  $k$ , while the  $H^1$ -semi-norm error is almost a constant times  $k^m h^m$ , all agreeing with Sect. 2.2. Only the last column needs some explanation. From  $k = 5\pi + 1$  to  $k = 10\pi + 1$  (and to  $k = 20\pi + 1$ , etc.),  $|e^h|_{H^1}$  experiences a drop at the same  $kh$  value. For sufficiently small  $h$ , the mixed source is actually well resolved. To understand the error drops as  $k$  increases, we go back to Sect. 2.2 and take a closer look at row 3-5 and column 3 of Fig. 1. It can be seen that the evanescent modes (with Fourier frequency  $\xi_n$  greater than the wavenumber  $k$ ) have a larger error than the propagating modes (with  $\xi_n < k$ ). Now let us plot the symbol errors when  $kh$  is fixed but  $k$  increases; see Fig. 2. We see that small  $k$  has a larger evanescent error. Those evanescent errors which dominate  $|e^h|_{H^1}$  simply decreases while  $k$  increases and  $kh$  is fixed. In Fig. 3, it is also seen that, for small values of  $kh$ , the round-off errors become apparent in both the 4th and 6th order schemes, indicating a smallest  $h$  usable in practice.

## References

- [1] Ivo M Babuska and Stefan A Sauter. Is the pollution effect of the FEM avoidable for the Helmholtz equation considering high wave numbers? *SIAM Journal on Numerical Analysis*, 34(6):2392–2423, 1997.
- [2] Pierre-Henri Cocquet, Martin J Gander, and Xueshuang Xiang. Closed form dispersion corrections including a real shifted wavenumber for finite difference discretizations of 2D constant coefficient Helmholtz problems. *SIAM Journal on Scientific Computing*, 43(1):A278–A308, 2021.
- [3] Arnaud Deraemaeker, Ivo Babuška, and Philippe Bouillard. Dispersion and pollution of the FEM solution for the Helmholtz equation in one, two and three dimensions. *International Journal for Numerical Methods in Engineering*, 46(4):471–499, 1999.
- [4] Vandana Dwarka and Cornelis Vuik. Pollution and accuracy of solutions of the Helmholtz equation: A novel perspective from the eigenvalues. *Journal of Computational and Applied Mathematics*, 395:113549, 2021.
- [5] Yiping Fu. Compact fourth-order finite difference schemes for Helmholtz equation with high wave numbers. *Journal of Computational Mathematics*, pages 98–111, 2008.
- [6] Christiaan C Stolk. A dispersion minimizing scheme for the 3-D Helmholtz equation based on ray theory. *Journal of Computational Physics*, 314:618–646, 2016.
- [7] Kun Wang and Yau Shu Wong. Pollution-free finite difference schemes for non-homogeneous Helmholtz equation. *International Journal of Numerical Analysis and Modeling*, 11(4), 2014.
- [8] Tingting Wu. A dispersion minimizing compact finite difference scheme for the 2D Helmholtz equation. *Journal of Computational and Applied Mathematics*, 311:497–512, 2017.

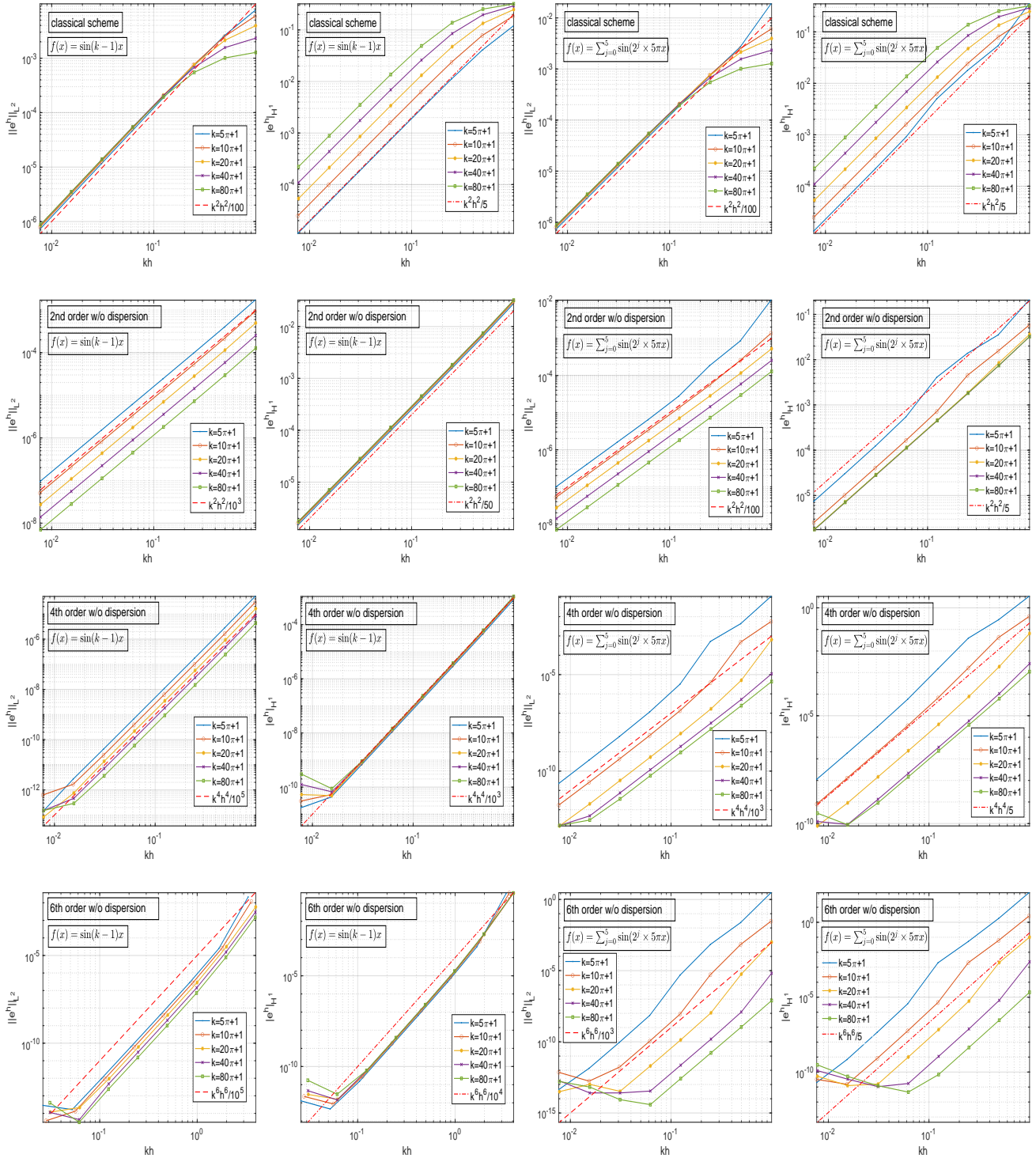


Figure 3: Numerical errors in 1D: monochromatic  $k$ -dependent source (col.1-2), mixed and fixed source (col.3-4).

(1dnum)